ANTICANCER RESEARCH *37*: 1263-1272 (2017)
doi:10.21873/anticanres.11443

Biparametric *versus* Multiparametric MRI with Non-endorectal Coil at 3T in the Detection and Localization of Prostate Cancer

MICHELE SCIALPI[1], ENRICO PROSPERI[2], ALFREDO D'ANDREA[3], EUGENIO MARTORANA[4], CORRADO MALASPINA[1], BARBARA PALUMBO[1], AGOSTINO ORLANDI[1], GIUSEPPE FALCONE[1], MICHELE MILIZIA[1], LUIGI MEARINI[5], MARIA CRISTINA AISA[6], PIETRO SCIALPI[7], CARLO DE DOMINCIS[8], GIAMPAOLO BIANCHI[4] and ANGELO SIDONI[2]

Divisions of [1]Radiology 2 and Nuclear Medicine, [5]Urology, and [6]Gynaecology, and [2]Section of Anatomic Pathology and Histology, Department of Surgical and Biomedical Sciences, S. Maria della Misericordia Hospital, Perugia University, Perugia, Italy; [3]Division of Radiology, San Giuseppe Moscati Hospital, Aversa, Italy; [4]Department of Urology, University of Modena, Modena, Italy; [7]Division of Urology, Portogruaro, Venice, Italy; [8]Department of Gynaecology and Obstetric Science and Urologic Science, La Sapienza University of Rome, Rome, Italy

Abstract. *Aim: To assess the sensitivity of biparametric magnetic resonance imaging (bpMRI) with non-endorectal coil in the detection and localization of index (dominant) and non-index lesions in patients suspected of having prostate cancer. Patients and Methods: We carried-out a retrospective analysis of multiparametric MRI (mpMRI) of 41 patients who underwent radical prostatectomy. Results of MRI for detection and localization of index and non-index lesions were correlated with those of histology. Results: No statistically significant difference in size was seen between tumor lesion at histology and index lesion at MRI. In 41 patients, a total of 131 tumors were identified at histology, while bpMRI (T2-weighted and diffusion-weighted MRI) approach detected 181 lesions. bpMRI gave 27.6% false-positives and 3.3% false-negatives. Sensitivity in lesion detection by bpMRI increased with lesion size assuming high values for lesions ≥10 mm. For bpMRI and mpMRI, the sensitivity for detecting index lesions was the same and equal: 100% in the peripheral zone 97.6% and 94.7% in the entire prostate and transitional zone, respectively. Conclusion: bpMRI can be used alternatively to mpMRI to detect and localize index prostate cancer.*

Correspondence to: Michele Scialpi, MD, Associate Professor of Radiology, Perugia University, [06156] S.M. della Misericordia Hospital, S. Andrea delle Fratte, 06156 Perugia, Italy. Tel: +39 075.5783507, Fax: +39 0755783488, e-mail: michelescialpi1@gmail.com

Key Words: Prostate cancer, detection, localization, biparametric MRI, diffusion-weighted imaging.

Detection of prostate cancer (PCa) within the prostate by imaging is relevant for appropriate decision making (biopsy or active surveillance). Multiparametric magnetic resonance imaging (mpMRI) [T2-weighted (T2W), diffusion-weighted (DW) and dynamic contrast-enhanced (DCE) MRI], in patients suspected of having PCa has revolutionized the conventional approach based on serum prostate-specific antigen (PSA) tests, digital rectal examination (DRE) and transrectal ultrasound (TRUS)-guided biopsy. It has emerged as an anatomical and functional imaging method that offers diagnostic accuracy in detecting, localizing, and staging PCa (1).

The American College of Radiology and the European Society of Urogenital Radiology prostate MRI working group have developed a Prostate Imaging Reporting and Data System (PIRADS) version 2.0 that provides extensive information on how to acquire, interpret, and report mpMRI of the prostate (1).

Among PIRADS 2.0 ambiguities and gaps (2), the limits of mpMRI such as the cost, the time required to complete the study (*e.g.* the use of gadolinium-based contrast agents requiring intravenous access or the use of an endorectal coil), and different technical parameters (*e.g.* field strength and b values) have to be considered. DCE MRI sequences have little effect on the detection of transition zone (TZ) lesions and variability in reader interpretation score, and have a secondary role to T2W and DW MRI (1). Recently, biparametric MRI (bpMRI), incorporating axial fat suppression T1-weighted (T1W), T2W and DW MRI series, has been proposed as an alternative method to mpMRI for detection and localization of PCa allowing an accurate stratification of patients (3-5).

Our aim was to assess the sensitivity of bpMRI with non-endorectal coil in the detection and localization of index (dominant) and non-index lesions and compare them with histology in patients with PCa after radical prostatectomy.

Patients and Methods

Patients. This retrospective study was approved by our Institutional Review Board (n. 1629/10). All patients gave written informed consent for MRI.

We retrospectively reviewed MRI of the prostate performed with a 3T system between January 2014 and December 2015 at our institution in 62 patients who underwent radical prostatectomy-proven PCa with a time interval between MRI and surgery ranging from 28 to 121 days (mean=63 days).

Patients who met the following inclusion criteria were selected: (a) 3T MRI with non-endorectal coil of the prostate, including T1W fat suppression, triplanar T2-weighted, DW MRI sequences with b values of 0-2,000 s/mm^2, and DCE MRI sequences; and (b) radical prostatectomy performed at our Institution with whole-mount step-section pathological tumor map availability.

Patients were excluded when (a) they had undergone PCa treatment, including hormone therapy or radiation; (b) MRI acquisition was incomplete or had imaging artifacts rendering the examination nondiagnostic or was obscured by hemorrhage-related prior biopsy; and (c) MRI was performed with an endorectal coil.

Our final study population consisted of 41 patients (mean age=64.5 years, range 53 to 78 years) with a mean serum PSA of 7.8 ng/dl (median=6.8 ng/dl, range=1.5-39.3 ng/dl), in whom 41 index tumors histologically diagnosed and originating in the peripheral zone (PZ) (n=22) or in the transitional zone (TZ) (n=19) were depicted as the index lesion (maximum diameter measured on the MRI sequence in which the lesion appeared better detected).

MRI was performed within 45 days before TRUS-guided biopsy in 21 patients and after a median of 40 days from TRUS-guided biopsy in 20 patients.

At histology, PCa was multifocal in 34 patients and monofocal in seven. The Gleason score (GS) was 6 (grade group 1) in 19 patients and ≥7 (grade group 2 or higher) in 22 patients. Excluding 36 PCa <5 mm, 131 PCa cases (index and non-index tumors) were considered at histology and correlated with index and non-index lesions found at MRI.

MRI protocol. All images were obtained immediately after intramuscular administration of 1 mg of butylscopolamine (Buscopan; Boehringer Ingelheim GmbH, Germany), injected intramuscularly to reduce peristalsis of the rectum.

All examinations were acquired on a 3T MRI system (Achieva; Philips Medical Systems Healthcare, Eindhoven, the Netherlands) equipped with a 16-channel torso phased-array *surface coil* (SENSE XL; Philips Medical Systems, Best, the Netherlands).

The protocol for prostate MRI included: a) axial T1W gradient-echo sequence with fat-suppression technique (THRIVE) imaging [repetition time (TR)=3.0 ms, echo time (TE)=1.5 ms; voxel= 1.4×1.4×1.4 mm^3; field of view (FOV)=35 cm; matrix= 252×201]; axial, sagittal and coronal T2W FSE imaging (TR=4.500-6.500 ms; TE=90 ms; slice thickness=3.0 mm; intersection gap=0; FOV=18 cm; matrix=212×212); b) axial DW [TR=3.100 ms; TE=102 ms; slice thickness=3.0 mm; exponential b values of 0, 750, 1,500 and 2,000 s/mm^2 with automatic calculation of apparent diffusion coefficient (ADC) maps; intersection ga*p*= 0; FOV=28-32 cm]; and c) axial DCE MRI using T1W THRIVE (TR=5.1 ms; TE=2.5 ms; voxel=1.5× 1.5×1.5mm^3; FOV=18 cm; matrix=120×116).

Data acquisition for DCE MRI began simultaneously with initiation of intravenous injection of gadopentetate dimeglumine (Gd-DTPA, Magnevist; Bayer Schering Pharma AG, Berlin, Germany) of 0.1 mmol/kg body weight at a rate of 3 ml/s via a power injector (Medrad, Warrendale, PA, USA), followed by a 40-ml saline flush at the same rate of Gd-DTPA injection. Multiphase DCE MRI was obtained every 12 s for 3 min without breath-holding.

Histopathological analysis. For all 41 patients, the reference standard for tumor localization was discriminated by using the step-section histological analysis of radical prostatectomy specimens, sliced from apex to base at 3-4-mm intervals in a plane perpendicular to the prostate urethra, and slices were placed on glass slides and stained with hematoxylin-eosin after paraffin embedding. For each patient, one of two dedicated genitourinary pathologists at our Institution, with more than 20 years of combined experience, verified histology and assigned a GS for each tumor focus outlined on the histology slides.

The pathologist further recorded the tumor location and size, tumor shape (regular or irregular borders), surgical margin, presence of lymph node metastases, presence of distant metastasis and final pathological stage in the pathological report. PCa was defined histopathologically according to the classification of the World Health Organization (WHO) in 2016 (6) and evaluated according to the 2016 International Society of Urological Pathology PCa grading (7).

If a lesion extended into more than one pathological slice, the areas of tumor foci on all slices were summed to obtain an estimate of the histopathological diameter of the whole lesion. Tumors that covered both zones, the TZ as well as the PZ, were considered to be TZ tumors if more than 70% of the tumor was in the TZ (8), all others were considered to be PZ tumors (9).

Pathologic-MRI evaluation and data analysis. The index tumor was outlined in each prostatectomy specimen by two pathologist (AS, EP) blinded to MRI. The criterion for the tumor lesion was that it had to be the largest or have the highest GS for the entire prostatectomy specimen (10, 11). For each index tumor, the greatest axial dimension was measured.

MR images were interpreted in consensus by two experienced radiologists (MS, ADA) in prostate MRI. They were aware that patients had PCa but were blinded to other clinical (rectal examination), biological (PSA value) and histopathological results (radical prostatectomy). Prostate MR images were reviewed to detect and to localize the index lesion (lesion largest on high b-value and inverted gray-scale DW MRI). Assessment of extracapsular extension was not taken into account in this study.

According to the literature (10, 12, 13) for detection of the index lesion within the prostate gland, the MRI criteria were: on T2W MRI: a well-circumscribed area of low signal intensity; on DW MRI and ADC map: well-circumscribed area of high signal intensity and low signal intensity, respectively; on DCE MRI: the diagnostic criteria included a focus of asymmetric, early and intense enhancement with rapid washout compared to background. In the lesion detection, we evaluated the MRI considering first DW MRI at high b-value and inverted gray-scale and ADC map; after we

Table I. *Cohen's k coefficient for T2-weighted (T2W), diffusion-weighted (DW), dynamic contrast-enhanced (DCE), biparametric MRI (bpMRI) and multiparametric MRI (mpMRI) in prostate cancer detection.*

		T2W	DW	DCE	bpMRI (T2W + DW)	mpMRI (T2W + DW + DCE)
Prostate	k	0.092	0.655	0.028	0.655	0.655
	CI	–0.079-0.263	0.0293-1	–0.028-0.0848	0.0293-1	0.0293-1
PZ	k	0.353	1	0.039	1	1
	CI	–0.166-0.872	1-1	–0.0617-0.189	1-1	1-1
TZ	k	0.078	0.0646	0.039	0.646	0.646
	CI	–0.0744-0.23	0.003-1	–0.0422-0.12	0.003-1	0.003-1

CI: Confidence interval. PZ: Peripheral zone. Transitional zone: TZ.

considered T2W MRI to confirm the low signal intensity of the lesion and its localization (PZ, TZ and base mid-gland and apex), DCE MRI was finally evaluated.

Tumor diameter was measured in consensus by two Radiologists on Picture Archiving and Communication System software. After detection and measurement, the tumor site was considered to match histological findings if the tumor depicted on the image was present in the same region of the prostate indicated in the prostatectomy specimen. A size ≥5 mm for correlation between histology and MRI was considered.

According to the PIRADS 2.0 version, in the localization of the index lesion, the segmentation model adapted from a European Consensus Meeting and the 2012 European Society of Urogenital Radiology Prostate MRI Guidelines was used employing 39 sectors/regions: 36 for the prostate, two for the seminal vesicles, and one for the external urethral sphincter (1). Any discrepancies between the two radiologists were resolved through a discussion by reaching a consensus.

Statistical analysis. Statistical analysis was performed using SPSS software (version 19.0; IBM Corp., Armonk, NY, USA) with the level of statistical significance set at $p<0.05$.

The index lesions detected by T2W, DW and DCE MRI alone or combined by T2W and DW MRI (bpMRI), or T2W, DW and DCE MRI (mpMRI) were correlated to tumor lesions at histology of the radical prostatectomy (standard reference) and potential differences or agreements were assessed using McNemar's test and the Cohen's kappa (k) coefficient, respectively.

Sensitivity for detection of the index lesion was calculated for T2W, DW and DCE MRI alone, and combined in bpMRI and mpMRI.

Statistical indicators [sensitivity, specificity, accuracy, positive predictive values (PPV) and negative predictive values (NPV)] of diagnostic performance of bpMRI were evaluated including all the lesions, both index and non-index lesions, identified and distributed, according to the size, into groups of ≥5, ≥7 and ≥10 mm. The ≥5 mm group included all the lesions detected, whereas the ≥7 and the ≥10 mm ones excluded lesions <7 and <10 mm, respectively. This approach progressively eliminated (in ascending grade) the smaller lesions with lower diagnostic relevance (1), from the statistical evaluation, in order to determine the limit of size with high values of test performance.

Non-neoplastic areas at histology and at bpMRI (no low signal intensity on T2W MRI and of no high signal intensity and no low signal intensity on DW and ADC, respectively), adjacent to the suspected lesions, were considered true-negatives.

Comparison and correlation between the size of index lesions detected by bpMRI and histological analysis were assessed using the Wilcoxon matched-pairs signed-rank test and the Spearman's rho rank correlation coefficient analysis, respectively.

The predictive accuracy of tumor aggressiveness by the index lesion size, measured with the histological and bpMRI approaches, was quantified as the area (AUC) under the receiver operating characteristics (ROC) curve. Analysis was performed by comparing index lesion size with GS=6 *vs*. GS ≥7.

Results

McNemar test demonstrated a significant statistical difference between results from histological analysis and both T2W ($p=0.001$) and DCE ($p<0.0001$) sequences, whereas no significant difference occurred with DW ($p=1$), bpMRI ($p=1$) and mpMRI ($p=1$).

Values of Cohen's k coefficient for DW, T2W, DCE, bpMRI and mpMRI are reported in Table I. In summary, relating to the reference standard, k values indicated a substantial agreement of DW and a slight agreement of T2W and DCE, in all data. In TZ, the agreement was substantial for DW and slight for T2W and DCE, whereas in PZ it was perfect, fair and slight for DW, T2W and DCE, respectively. Using the combined approaches, bpMRI and mpMRI, a perfect agreement was demonstrated in PZ, whereas it was substantial in the entire prostate and in TZ, in both approaches. DW MRI correctly detected 40 out of 41 index lesions; one false-negative was inherent to a lesion detected controlaterally to the index lesion (erroneously considered smaller due to its oblique position on axial DW MRI). The sensitivity of DW MRI was 97.6% in all data, whereas it was 100% and 94.7% for PZ and TZ, respectively. The sensitivity of T2W and of DCE MRI for all data, TZ and PZ was 68.3, 47.4 and 86.4%, and 39.02, 31.6 and 45.4%, respectively. In both types of combined MRI (bpMRI and mpMRI) the sensitivity was the same and was 100% in PZ and 97.6 and 94.7% in the entire prostate and TZ, respectively.

Representative cases of PCa at mpMRI and bpMRI with pathologic correlation are shown in Figures 1 and 2.

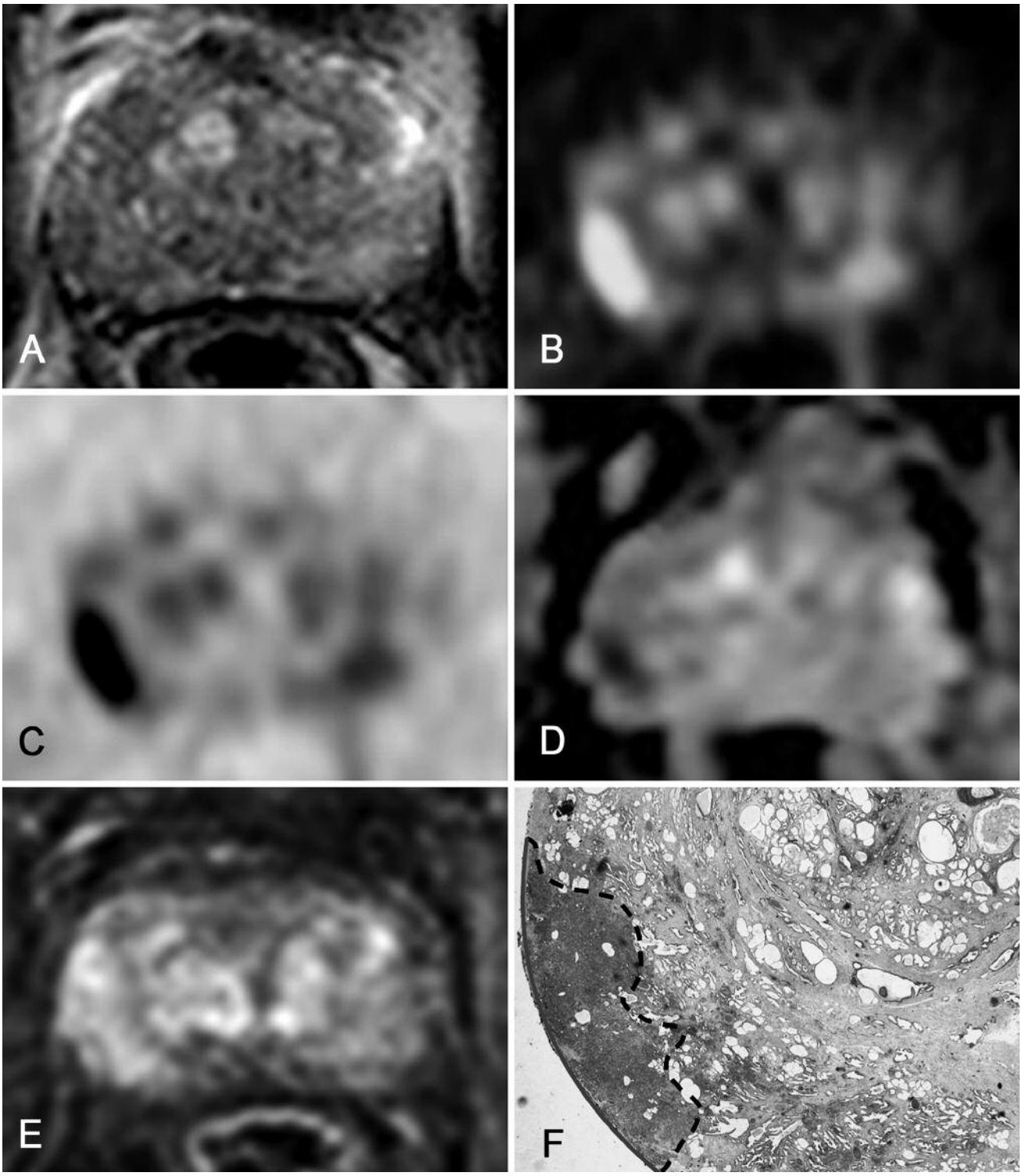

Figure 1. *70 year-old, with PSA of 5.1 ng/dl without previous biopsy, with lesion affecting the peripheral zone in the right side of the middle gland. The lesion appears homogeneously hypointense on T2-weighted (a), hyperintense and hypointense on high b-value (2.000 s/mm^2) (B) and inverted gray-scale (C) diffusion-weighted magnetic resonance imaging, respectively, and moderately hypointense on the apparent diffusion coefficient map (D) indicating restricted diffusion. On dynamic contrast enhanced the lesion shows a substantially similar enhancement to the adjacent peripheral zone and stromal nodules in the transitional zone (E). The histological resection (F) (hematoxylin-eosin; ×1.5) confirms a Gleason Score 6 tumor in the peripheral zone of the right lobe of the gland, with a positive surgical margin (dotted line).*

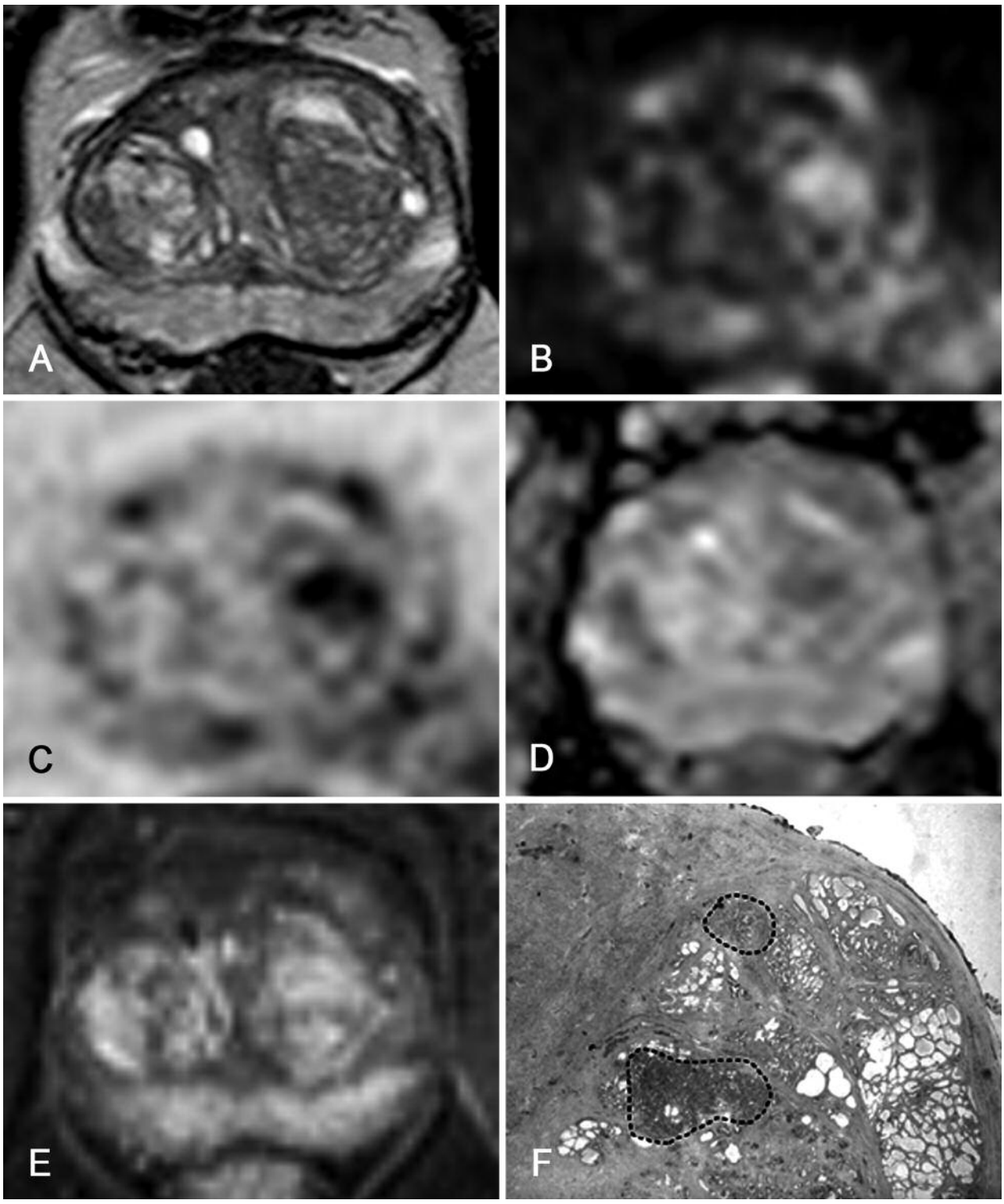

Figure 2. *63 year-old, with PSA of 13.9 ng/dl with previous biopsy, with lesion lesion affecting the transitional zone in the left side of the middle gland. The lesion appears hypointense on T2-weighted (A), hyperintense and hypointense on high b-value (2.000 s/mm^2) (B) and inverted gray-scale (C) diffusion-weighted magnetic resonance imaging, respectively, and moderately hypointense on the apparent diffusion coefficient map (D), indicating restricted diffusion. On dynamic contrast enhanced MRI (E) the lesion is indistinguishable from the stromal nodules in the transitional zone. The histologic resection (f) (hematoxylin-eosin; ×1.5) confirms a Gleason Score 7 tumor in the transitional zone (bottom of the figure, index lesion) in the left lobule of the gland. Note another small Gleason Score 6 tumor in the peripheral zone (top of the figure).*

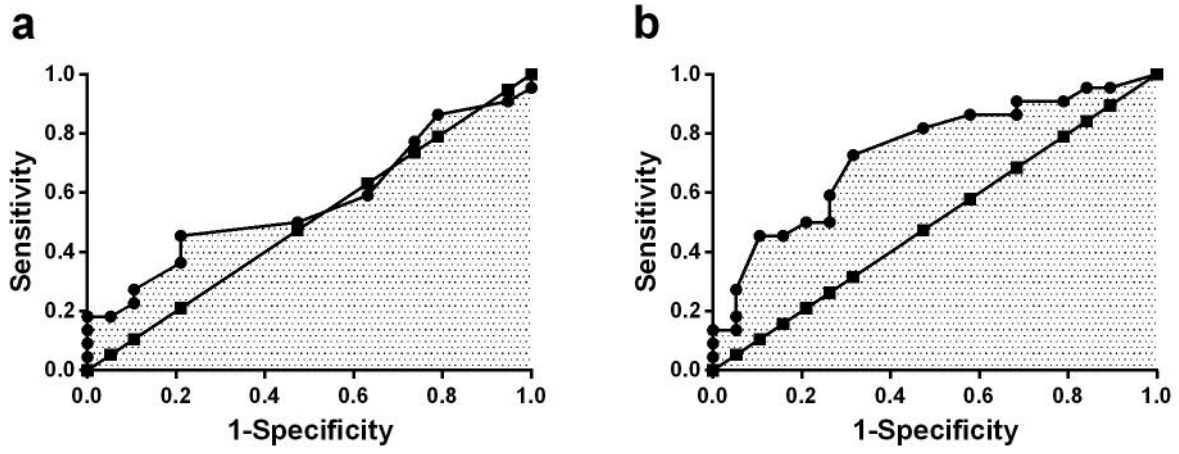

Figure 3. *Areas under the receiver operating characteristic curves for the index lesion size detected with biparametric magnetic resonance imaging (a) and histological (b) approaches.*

Considering the low sensitivity of DCE in the detection of the index lesion, we evaluated the sensitivity of bpMRI for all the lesions (index and non-index) detected. In 41 patients, a total of 131 and 181 lesions was determined by histology and bpMRI, respectively. bpMRI gave 27.6% false-positives and 3.3% false-negatives.

As false-positives and false-negatives occurred, in order to define from which limit of lesion size the diagnostic performance of bpMRI was high, data were distributed into groups of ≥5, ≥7 and ≥10 mm and the main statistical indicators were calculated (Table II). Sensitivity, specificity, accuracy, PPV and NPV of bpMRI increased with the size of the lesion, assuming high values for lesions ≥10 mm.

The size of tumor lesions at histology ranged from 5 to 31 mm [mean=15.63 mm, SD=6.18 mm; median=15 mm, interquartile range (IQR)=12-20 mm]. The index lesion measured on high b-value DW sequences ranged from 6 to 33 mm (mean=15.71 mm, SD=5.45 mm, median=14 mm, IQR=12.5-19 mm). No significant differences between the two groups were seen (data not shown) and their correlation (rho= 0.702, strong) was statistically significant ($p<0.0001$).

Size of GS=6 (grade group 1) lesions (n=19) at histology ranged from 5 to 25 mm (mean=3.16 mm, SD=5.26 mm, median=13 mm, IQR=10-17 mm). The index lesion measured on high b-value DW sequences ranged from 9 to 22 mm (mean=14.47 mm, SD=3.6 mm, median=14 mm, IQR=12-15 mm). Their correlation (rho= 0.589, moderate) was statistically significant ($p<0.008$).

Size of GS≥7 (grade group 2 or higher) lesions (n=22) at histology ranged from 5 to 31 mm (mean=17.7 mm, SD=6.2 mm, median=17 mm, IQR=14-21 mm). The index lesion measured on axial DWI/ADC sequences ranged from 6 to 33 mm (mean=16.7 mm, SD=6.5 mm, median=14.50 mm, IQR=12.75-20.25 mm). Their correlation (rho=0.809, very strong) was statistically significant ($p<0.0001$).

Table II. *Statistical indicators of diagnostic performance of biparametric MRI.*

	Lesion size		
	≥5 mm	≥7 mm	≥10 mm
Sensitivity	0.956	0.987	0.982
Specificity	0.783	0.748	0.858
PPV	0.848	0.868	0.956
NPV	0.724	0.601	0.848
Accuracy	0.968	0.994	0.994

NPV: Negative predictive values; PPV: Positive Predictive values.

In order to establish a possible predictive accuracy of tumor aggressiveness by the index lesion size, we evaluated the areas under the ROC curves for the index lesion size detected with bpMRI and with histological approach (Figure 3). Conversely to the results from histology (AUC=0.736, $p=0.01$), bpMRI in the lesion size detection was not able to discriminate by the aggressiveness of tumor (AUC=0.569, $p=0.44$).

Discussion

The introduction of MRI into clinical practice has revolutionized the conventional approach (*i.e.* DRE and TRUS) in patients suspected of having PCa (14-16). Both DRE and TRUS are suboptimal for the diagnosis of PCa; particularly, DRE has shown to be a poor predictor of tumor location and extent (17), and the accuracy for local staging by DRE is lower than that by TRUS (18). The sensitivity of

TRUS in the detection of PCa is low (19); the only indicator for diagnosis of PCa remains the PSA level.

mpMRI, developed and tested as an anatomical and functional evaluation of the prostate, is considered the most sensitive radiological tool for PCa detection and characterization of higher-risk disease (17), allowing a new, more rational, approach to PCa investigation and selection of men for closer monitoring or diagnostic biopsy.

In the current PIRADS 2.0, DW and T2W MRI are the dominant sequences for detection and localization of PCa in the PZ and TZ respectively; DCE MRI plays only a minor role in determining the PIRADS assessment category, and has a secondary role to T2W and DW MRI (each lesion being assigned a positive or negative score) in PCa detection and localization (1).

Several studies have demonstrated a significantly better accuracy for PCa detection of DWI compared to T2W MRI (20-22), especially in PZ (21).

In the detection of PCa, T2W and DW, T2W and DCE and all three parameters combined as mpMRI were significantly more accurate than T2W alone; however, bpMRI was significantly greater in accuracy than T2W and DCE alone and all three parameters combined (22). In addition, the diagnostic value of bpMRI in men, with or without previous biopsy, and combined with PSA, has been validated, resulting in an improved accuracy for detecting clinically-significant PCa and to direct biopsy needles under TRUS guidance, after MRI–ultrasonography fusion (5, 23, 24).

In our study, we investigated the value of bpMRI compared to mpMRI in the detection and localization of PCa in patients with PSA abnormalities with or without previous negative biopsies submitted to radical prostatectomy.

For the index lesion detection, we used T2W, DW and DCE MRI alone or combined in bpMRI (T2W and DW MRI) or mpMRI (T2W, DW and DCE MRI). Compared to the histological findings (standard reference), DW MRI showed no statistically significant difference and a substantial agreement in all data in TZ, or a perfect agreement in PZ. On the contrary, T2W and DCE exhibited significant differences from histological results, as well as a slight/fair agreement in all data, TZ and PZ. The agreement of DW, T2W and DCE, alone, was in the order: DW >>T2W > DCE. In the combined MRI approaches, the agreement of bpMRI and mpMRI (which corresponded to the value of DW alone) was identical, indicating that DCE sequence in mpMRI did not contribute to detection of the index lesion in PZ and in TZ. Analogous trends were observed for the sensitivity of DW, T2W, DCE alone, in bpMRI and mpMRI, further indicating that DCE sequence in mpMRI did not provide additional evidence for the index lesion detection in PZ and in TZ.

All the above data were in disagreement with PIRADS 2.0 (1).

One case of false-negative of index lesion detection occurred with DW MRI analysis. However, it can be assumed that with this approach all the index lesions evidenced by histology were substantially detected. A lenticular lesion (false-negative), located in TZ, was indeed erroneously considered smaller, due to its oblique position on axial DW MRI, and consequently misinterpreted.

Concerning the examination of all lesions (both index and non-index), a number of false-negatives (low) and false-positives (high) occurred. False-negatives concerned <7 mm lesions, false-positives were mostly related to <10 mm lesions. Interestingly, as a consequence, the sensitivity, specificity, accuracy, PPV and NPV of bpMRI increased with the size of the lesion, assuming high values for lesions ≥10 mm. This can potentially reduce the risk of both false-positives and false-negatives in the group of clinically significant lesions (GS ≥7). In PIRADS 2.0, indeed, a cut-off value of 15 mm to discriminate tumor aggressiveness has been reported (1). Additionally, the very strong correlation between lesion size from histology and from bpMRI of GS ≥7 groups, as well as the 25% percentile value >10 mm, for the lesion size detected by bpMRI in the GS ≥7 group, are in support of this hypothesis. ROC curve analysis of bpMRI data failed to provide additional evidence in this regard. However, it is plausible to postulate that the small number of patients under investigation significantly influenced the result.

Our study had several limitations. Firstly, it was a retrospective study with a relatively small series, confirming the diagnostic performance of the bpMRI. For this reason, further prospective studies with a larger number of patients should be performed to validate these results. Secondly, for the correlation analysis, we did not select all patients who had biopsy after bpMRI in order to reduce false-positives (high-grade prostatic intraepitelial neoplasia, chronic prostatitis, non-infective granulomatous prostatitis and stromal hyperplasia) and false-negative lesions by bpMRI: in our study 21 patients had biopsy before MRI. The false-negatives were related to small lesions (≤7 mm); however, as reported elsewhere (25), 5 mm and 7 mm lesions were demonstrated at histology to be benign lesions in 87.5% and 86.2%, respectively, or low-grade GS 6 PCa (12.5% and 13.8% and respectively) on lesion-specific targeted biopsies. In addition, the slow growth rate of these small index lesions on serial mpMRI indicates a surveillance interval of at least 2 years without significant change (25). Thirdly, we used a non-weighted score for MRI and we were unable to use PI-RADS to compare the two kinds of MRIs. We suggest that patients suspected of having PCa [focal rounded, lenticular or irregular, heterogeneous or homogeneous, mild/moderately or markedly hypointense on T2W MRI and diffusion restriction (hyperintense on DW MRI and hypointense on ADC maps)] with index lesion ≥10 mm in maximum diameter, are candidates for targeted biopsy. Further improvement to the

lesion diameter for accurate management is represented by bpMRI with lesion volume calculation (26).

In conclusion, bpMRI is sufficient for the detection and localization of the index PCa. It offers a scanning in less time than mpMRI (approximately 15-20 min *vs*. 25-30 min), with reduced costs (contrast medium is eliminated and encorectal coil is not used) and with a diagnostic value comparable to that of mpMRI, allows for anadequate patient management.

Further studies are needed to evaluate the usefulness of bpMRI in clinical practice.

Conflicts of Interest

The Authors declare that they have no competing interests.

References

1 Prostate Imaging Reporting and Data System (PI-RADS) Reston (VA): American College of Radiology. http://www. acr.org/Quality-Safety/Resources/PIRADS/2015.

2 Rosenkrantz AB, Oto A, Turkbey B and Westphalen AC: Prostate imaging reporting and data system (PI-RADS), version 2: a critical look. Am J Roentgenol *206*: 1179-1183, 2016.

3 Scialpi M, Falcone G, Scialpi P and D'Andrea A: Biparametric MRI: a further improvement to PIRADS 2.0? Diagn Interv Radiol *22*: 297-298, 2016.

4 Scialpi M, Martorana E and D'Andrea A: Standardizing biparametric MRI to simplify and improve Prostate Imaging Reporting and Data System, version 2, in prostate cancer management. (letter) Am J Roentgenol *207*: W74-W75, 2016.

5 Rais-Bahrami S, Siddiqui MM, Vourganti S, Turkbey B, Rastinehad AR, Stamatakis L, Truong H, Walton-Diaz A, Hoang AN, Nix JW, Merino MJ, Wood BJ, Simon RM, Choyke PL and Pinto PA: Diagnostic value of biparametric magnetic resonance imaging (MRI) as an adjunct to prostate-specific antigen (PSA)-based detection of prostate cancer in men without prior biopsies BJU Int *115(3)*: 381-388, 2015.

6 WHO classification of tumours of the urinary system and male genital organs. H Roch, PA Murphrey, TR Ulbright, Ve Reuter (eds.), Lyon, IARC, 2016.

7 Egevad L, Delahunt B, Evans AJ, Kench JG, Kristiansen G, Leite KR, Samaratunga H and Srigley JR: Grading of prostate cancer. J Surg Pathol *40*: 858-861, 2016.

8 McNealJE, RedwineEA, Freiha FS and StameyTA: Zonal distribution of prostatic adenocarcinoma. Correlation with histologic pattern and direction of spread. Am J Surg Pathol *12*: 897-906, 1988.

9 Kobus T, Vos PC, Hambrock T, De Rooij M, Hulsbergen-Van de Kaa CA, Barentsz JO, Heerschap A and Scheenen TW: Prostate cancer aggressiveness: *in vivo* assessment of MR spectroscopy and diffusion-weighted imaging at 3 T. Radiology *265*: 457-467, 2012.

10 Turkbey B, Pinto PA, Mani H, Bernardo M, Pang Y, McKinney YL, Khurana K, Ravizzini GC, Albert PS, Merino MJ and Choyke PL: Prostate Cancer: value of multiparametric MR imaging at 3 T for detection – histopatologic correlation. Radiology *255(1)*: 89-99, 2010.

11 Lee DJ, Ahmed HU, Moore CM, Emberton M and Ehdaie B: Multiparametric magnetic resonance imaging in the management and diagnosis of prostate cancer: current applications and strategies. Curr Urol Rep *15(3)*: 390-400, 2014.

12 Turkbey B, Pinto PA, Mani H, Bernardo M, Pang Y, McKinney YL, Khurana K, Ravizzini GC, Albert PS, Merino MJ and Choyke PL: Multiparametric 3T prostate magnetic resonance maging to detect cancer:histopathological correlation using prostatectomy specimens processed in customized magnetic resonance imaging based molds. J Urol *186*: 1818-1824, 2011.

13 Turkbey B, Thomasson D, Pang Y, Bernardo M and Choyke PL: The role of dynamic contrast-enhanced MRI in cancer diagnosis and treatment. Diagn Interv Radiol *16*: 186-1927, 2010.

14 Turkbey B, Mani H, Aras O, Ho J, Hoang A, Rastinehad AR, Agarwal H, Shah V, Bernardo M, Pang Y, Daar D, McKinney YL, Linehan WM, Kaushal A, Merino MJ, Wood BJ, Pinto PA and Choyke PL: Prostate cancer: can multiparametric MR imaging help identify patients who are candidates for active surveillance? Radiology *268*: 144-152, 2013.

15 Rastinehad AR, Baccala AA Jr, Chung PH, Proano JM, Kruecker J, Xu S, Locklin JK, Turkbey B, Shih J, Bratslavsky G, Linehan WM, Glossop ND, Yan P, Kadoury S, Choyke PL, Wood BJ and Pinto PA.: D'Amico risk stratification correlates with degree of suspicion of prostate cancer on multiparametric magnetic resonance imaging. J Urol *185*: 815-820, 2011.

16 Stamatakis L, Siddiqui MM, Nix JW, Logan J, Rais-Bahrami S, Walton-Diaz A, Hoang AN, Vourganti S, Truong H, Shuch B, Parnes HL, Turkbey B, Choyke PL, Wood BJ, Simon RM and Pinto PA: Accuracy of multiparametric magnetic resonance imaging in confirming eligibility for active surveillance for men with prostate cancer. Cancer *119*: 3359-3366, 2013.

17 Obek C, Louis P, Civantos F and Soloway MS: Comparison of digital rectal examination and biopsy results with the radical prostatectomy specimen. J Urol *161(2)*: 494-498, 1999.

18 Presti JC Jr, Hricak H, Narayan PA, Shinohara K, White S and Carroll PR: Local staging of prostatic carcinoma: comparison of transrectal sonography and endorectal MR imaging. Am J Roentgenol *166(1)*: 103-108, 1996.

19 Fütterer JJ,Verma S,Hambrock T,Yakar D and Barentsz JO: High-risk prostate cancer: value of multi- modality 3T MRI-guided biopsies after previous negative biopsies. Abdom Imaging *37(5)*: 892-896, 2012.

20 Miao H, Fukatsu H and Ishigaki T: Prostate cancer detection with 3-T MRI: Comparison of diffusion- weighted and T2-weighted imaging. Eur J Radiol *61*: 297-302, 2007.

21 Haider MA, van der Kwast TH, Tanguay J, Evans AJ, Hashmi AT, Lockwood G and Trachtenberg J: Combined T2-weighted and diffusion-weighted MRI for localization of prostate cancer. Am J Roentgenol *189*: 323-328, 2007.

22 Delongchamps NB, Rouanne M, Flam T, Beuvon F, Liberatore M, Zerbib M and Cornud F: Multiparametric magnetic resonance imaging for the detection and localization of prostate cancer: combination of T2-weighted, dynamic contrast-enhanced and diffusion-weighted imaging. BJU Int *107(9)*: 1411-1418, 2011.

23 Radtke JP, Boxler S, Kuru TH, Wolf MB, Alt CD, Popeneciu IV, Steinemann S, Huettenbrink C, Bergstraesser-Gasch C, Klein T, Kesch C, Roethke M, Becker N, Roth W, Schlemmer HP, Hohenfellner M and Hadaschik BA: Improved detection of

anterior fibromuscular stroma and transition zone prostate cancer using biparametric and multiparametric MRI with MRI-targeted biopsy and MRI-US fusion guidance. Prostate Cancer Prostatic Dis *18*: 288-296, 2015.

24 Fascelli M, Rais-Bahrami S, Sankineni S, Brown AM, George AK, Ho R, Frye T, Kilchevsky A, Chelluri R, Abboud S, Siddiqui MM, Merino MJ, Wood BJ, Choyke PL, Pinto PA and Turkbey B: Combined biparametric prostate magnetic resonance imaging and prostate-specific antigen in the detection of prostate cancer: a validation study in a biopsy-naive patient population. Urology *88*: 125-134, 2016.

25 Rais-Bahrami S,Türkbey B, Rastinehad AR, Walton-Diaz A, Hoang AN, Siddiqui MM, Stamatakis L, Truong H, Nix JW, Vourganti S, Grant KB, Merino MJ, Choyke PL and Pinto PA: Natural history of small index lesions suspicious for prostate cancer on multiparametric MRI: recommendations for interval imaging follow-up. Diagn Interv Radiol *20(4)*: 293-298, 2014.

26 Martorana E, Pirola GM, Scialpi M, Micali S, Iseppi A, Bonetti LR, Kaleci S, Torricelli P and Bianchi G: Lesion volume predicts prostate cancer risk and aggressiveness: validation of its value alone and matched with prostate imaging reporting and data system score. BJU Int DOI:10.1111/bju.13649, 2016 [Epub ahead of print].

Received October 30, 2016
Revised November 17, 2016
Accepted December 6, 2016